



Article

Investigating Antibody Reactivity to the Intestinal Microbiome in Severe Myalgic Encephalomyelitis/Chronic Fatigue Syndrome (ME/CFS): A Feasibility Study

Katharine A. Seton ¹, Marianne Defernez ¹, Andrea Telatin ¹, Sumeet K. Tiwari ¹, George M. Savva ¹, Antonietta Hayhoe ¹, Alistair Noble ², Ana L. S. de Carvalho-KoK ³, Steve A. James ¹, Amolak Bansal ⁴, Thomas Wileman ^{1,5} and Simon R. Carding ^{1,5,*}

¹ Quadram Institute Bioscience, Norwich Research Park, Norwich NR4 7UQ, UK; katharine.seton@quadram.ac.uk (K.A.S.); andrea.telatin@quadram.ac.uk (A.T.); sumeet.tiwari@quadram.ac.uk (S.K.T.); george.savva@quadram.ac.uk (G.M.S.); antonietta.hayhoe@quadram.ac.uk (A.H.); steve.james@quadram.ac.uk (S.A.J.); tom.wileman@quadram.ac.uk (T.W.)

² The Pirbright Institute, Woking GU24 0NF, UK; alistair.noble@pirbright.ac.uk

³ Experimental Arthritis Treatment Centre for Children, University of Liverpool, Liverpool L12 2AP, UK; a.serafim-de-carvalho-kok@liverpool.ac.uk

⁴ Spire St Anthony's Hospital, Sutton SM3 9DW, UK; asbansal1000@yahoo.com

⁵ Norwich Medical School, University of East Anglia, Norwich NR4 7TJ, UK

* Correspondence: simon.carding@quadram.ac.uk

Abstract: Myalgic encephalomyelitis/chronic fatigue syndrome (ME/CFS) is a multisystemic disease of unknown aetiology that is characterised by disabling chronic fatigue and involves both the immune and gastrointestinal (GI) systems. Patients display alterations in GI microbiome with a significant proportion experiencing GI discomfort and pain and elevated blood biomarkers for altered intestinal permeability compared with healthy individuals. To investigate a possible GI origin of ME/CFS we designed a feasibility study to test the hypothesis that ME/CFS pathogenesis is a consequence of increased intestinal permeability that results in microbial translocation and a breakdown in immune tolerance leading to generation of antibodies reactive to indigenous intestinal microbes. Secretory immunoglobulin (Ig) A and serum IgG levels and reactivity to intestinal microbes were assessed in five pairs of severe ME/CFS patients and matched same-household healthy controls. For profiling serum IgG, we developed IgG-Seq which combines flow-cytometry based bacterial cell sorting and metagenomics to detect mucosal IgG reactivity to the microbiome. We uncovered evidence for immune dysfunction in severe ME/CFS patients that was characterised by reduced capacity and reactivity of serum IgG to stool microbes, irrespective of their source. This study provides the rationale for additional studies in larger cohorts of ME/CFS patients to further explore immune–microbiome interactions.

Keywords: myalgic encephalomyelitis/chronic fatigue syndrome (ME/CFS); antibodies; immunoglobulin G; immunoglobulin A; microbiome; autologous; heterologous; immune tolerance; leaky gut



Citation: Seton, K.A.; Defernez, M.; Telatin, A.; Tiwari, S.K.; Savva, G.M.; Hayhoe, A.; Noble, A.; de Carvalho-KoK, A.L.S.; James, S.A.; Bansal, A.; et al. Investigating Antibody Reactivity to the Intestinal Microbiome in Severe Myalgic Encephalomyelitis/Chronic Fatigue Syndrome (ME/CFS): A Feasibility Study. *Int. J. Mol. Sci.* **2023**, *24*, 15316. <https://doi.org/10.3390/ijms242015316>

Academic Editor: Vlatka Sotosek

Received: 12 September 2023

Revised: 3 October 2023

Accepted: 12 October 2023

Published: 18 October 2023



Copyright: © 2023 by the authors. Licensee MDPI, Basel, Switzerland. This article is an open access article distributed under the terms and conditions of the Creative Commons Attribution (CC BY) license (<https://creativecommons.org/licenses/by/4.0/>).

1. Introduction

Myalgic encephalomyelitis/chronic fatigue syndrome (ME/CFS) is characterised by disabling fatigue and autonomic, muscular, cognitive, neurological and immune symptoms that leave patients unable to undertake their pre-morbid work, education, exercise and social activities [1]. A quarter of diagnosed patients are house- or bedbound [2] and less than 5% ever recover their pre-morbid activity levels [3]. A meta-analysis based on 45 studies estimated an average population prevalence of 0.68% (95% CI = 0.48 to 0.97) [4]. However, these estimates vary considerably by population and case definition [4]. The prevalence is anticipated to rise following the COVID-19 pandemic as there is clinical

overlap between long COVID patients and ME/CFS patients, with some long COVID patients meeting the ME/CFS diagnostic criteria [5]. The most common trigger of ME/CFS is an infection, whilst other reported triggers include physical or mental trauma and toxin exposure [3].

Several factors have been implicated in ME/CFS pathogenesis involving the immune (autoimmunity, inflammation and chronic infection), gastrointestinal (GI), neurological, endocrine and metabolic systems [6]. Between 38 and 92% of ME/CFS patients report co-morbid GI disturbances such as irritable bowel syndrome (IBS) [3,7–9] and 35% of patients take medication for GI disturbances including pro- and prebiotics, digestive enzymes and sodium bicarbonate [3]. The high co-occurrence of ME/CFS and IBS suggests possible involvement of the intestinal microbiome. Consistent with this possibility, several studies have reported changes in the community structure of the stool microbiome of ME/CFS patients exemplified by reduced diversity [8] and decreased abundance of short-chain, fatty acid-producing bacterial species [8–12]. ME/CFS patients also have elevated biomarkers associated with increased intestinal permeability [8,13,14]. Intestinal inflammation and increased permeability can compromise immune and microbial tolerance (defined as a state of hypo responsiveness to indigenous intestinal microbes) [15], leading to hyperreactivity and serum antibody production to indigenous intestinal microbes [16]; this can pre-stage autoimmune disease [17]. Of note, ME/CFS patients displaying increased intestinal permeability have a higher incidence of serotonin autoimmunity [18].

Based upon these observations, we hypothesised that ME/CFS pathology is a consequence of the breakdown in immune tolerance resulting from the increased intestinal permeability and microbial translocation that leads to generation of antibodies reactive to indigenous intestinal microbes. In support of this proposal, a previous study found that, compared with healthy controls, ME/CFS patients had abnormally high levels of IgA and IgM produced in response to a panel of seven gram-negative enterobacteria [13]. However, this small panel of microbes does not reflect the complexity of the intestinal microbiota which comprises 300–500 bacterial species as well as viruses, archaea and fungi [19]. In addition, IgM antibodies have low specificity for antigens [20] and IgA is primarily produced at mucosal sites [21]. Serum IgG reactivity to the microbiome in ME/CFS patients has recently been investigated using phage immunoprecipitation sequencing (PhIP-Seq) to screen IgG reactivity to 244,000 bacterial and viral epitopes [22]. This study is, however, restricted to identifying antibody reactivity to peptide antigens and cannot detect reactivity to the immunogenic glycoproteins and lipoproteins that decorate the outer membrane and surface of bacterial cells, viruses and fungi [23]. Furthermore, none of the approaches used to date provide information on whether immune tolerance to indigenous intestinal microbes is lost in ME/CFS.

To begin to address this important question and assess the systemic humoral immune response to indigenous microbes, we employed 'IgG-Seq'; a method that combines flow cytometry-based bacterial cell sorting and microbial sequencing to detect systemic IgG reactivity to the microbiome and has previously been performed on both mouse and human samples [24–30].

We designed a pilot study with a small cohort of severe ME/CFS patients and healthy controls from the same households. The difficulty in accessing housebound or bedbound patients is a major obstacle to understanding the pathophysiology and aetiology of ME/CFS and is why only 0.5% of ME/CFS research is undertaken in severely affected patients [2]. One aim of this study, therefore, was to assess the feasibility and identify potential barriers to including severe ME/CFS patients in research, particularly in the context of the collection of biological samples.

2. Results

2.1. Recruiting Severe ME/CFS Patients and Same-Household Controls

Study participants were recruited from the CFS clinic at Epsom and St Helier University Hospitals (ESTH), Carshalton, UK, and the ME/CFS service at the East Coast

Community Healthcare Centre (ECCHC), Lowestoft, UK, which together had 3812 registered patients. Recruitment began in October 2017, with the intention of recruiting ten severe house or bedbound ME/CFS patients and ceased in April 2020 due to the COVID-19 pandemic. Thirty-six patients were invited to the study with a response rate of 58.3% (Figure S1). Of those who responded, 42.9% were ineligible due to either the absence of a household control (n = 4), failure to meet other inclusion criteria (n = 4) or were unable to provide written informed consent (n = 1). Of the 12 eligible pairs of participants, 6 provided informed consent. The consenting appointments for the other six eligible participants were delayed either due to patients rescheduling their appointments when feeling unwell, or the non-availability of phlebotomists to attend home visits. Consequently, consenting appointments were delayed by up to 12 months for participants, by which point three patients either saw their health further deteriorate preventing them from participating in the study, or acquired an additional health complication that excluded them from the study. We received no further communication from the remaining three pairs.

2.2. Study Population Characteristics

Samples were collected from five pairs of participants; one pair consented immediately prior to the COVID-19 pandemic which prevented us from obtaining their samples (Table 1). The recruited patients comprised four females and one male (mean age 33.8 years; standard deviation (SD) 13.8). There was clinical heterogeneity amongst patients, with variation in the age at which ME/CFS onset occurred, length of illness and symptom severity. Three patients reported ME/CFS onset following a viral infection, one following vaccination and one following surgery. IBS was reported in all patients but in none of their matched household controls. Same-household healthy controls included four males and one female (mean age 40.4 years; SD 16.7) who were the carers and spouse (n = 3), parent (n = 1) or sibling (n = 1) of the patients.

Table 1. Severe ME/CFS clinical characteristics.

	Participants Affected (%)	Mean (SD)	Range
Age of ME/CFS onset (years)	-	25.0 (9.34)	12–38
Length of ME/CFS (years)	-	8.4 (6.83)	2–21
Symptoms			
Post exertional malaise	100	-	-
Non-restorative sleep	100	-	-
Headaches of a new onset, pattern and severity	80	-	-
Recurrent sore throat with enlarged glands in neck	40	-	-
Impaired concentration	100	-	-
Impaired memory	80	-	-
Joint pain	60	-	-
Muscle pain	80	-	-
Visual and/or auditory hypersensitivity	100	-	-
Irritable bowel syndrome	100	-	-
Questionnaire (maximum score)			
Shortened SF-36 (30) *	-	11.0 (1.73)	10–14
Chalder fatigue–physical (28) *	-	24.0 (3.67)	18–27
Chalder fatigue–mental (16) *	-	13.5 (1.12)	12–15
HADS–anxiety (21) *	-	7.8 (4.55)	3–15
HADS–depression (21) *	-	6.5 (5.50)	3–16
Self-efficacy (60) **	-	12.0 (7.35)	3–21
Visual analogue (100) *	-	62.5 (36.31)	0–90
Epworth sleepiness (24) ***	-	7.5 (14)	1–14

* Questionnaire completed by 4 patients. ** questionnaire completed by 3 patients. *** questionnaire completed by 2 patients.

2.3. Stool Consistency Does Not Separate Severe ME/CFS Patients with IBS from Matched Household Controls without IBS

Despite all ME/CFS patients and no household controls reporting IBS, there was no evidence for a difference in consistency of the collected stool samples between patients and controls, as measured by the Bristol stool form scale (BSFS) or by water content

(Figure S2A,B). Three controls had abnormally loose stools (BSFS 5–7) indicative of diarrhoea and one control had an abnormally hard stool (BSFS 2) indicative of constipation. In contrast, two patients had stool samples defined as having a healthy consistency (BSFS 3–4), one patient had an abnormally loose stool (BSFS 5) and two patients had abnormally hard stools (BSFS 1–2).

2.4. Assessment of Secretory IgA (sIgA) in Stool

The concentrations of microbe bound IgA1/2 (Figure 1A) and free IgA1/2 (Figure 1B) were measured by enzyme linked immunosorbent assay (ELISA) with no evidence of a significant difference between severe ME/CFS patients and their matched household controls. Flow cytometry was used to determine the distribution of sIgA coating on stool microbes (Figure 2A,B). When comparing the proportion of stool microbes coated by sIgA there was no evidence of any differences between patients and matched controls (Figure 2C). Based on the microbial load of stool samples (Figure S3) the relative quantification of sIgA bound microbes was converted to absolute values which again revealed no evidence of differences between patients and matched controls in the quantity of sIgA coated microbes within stool samples (Figure 2D).

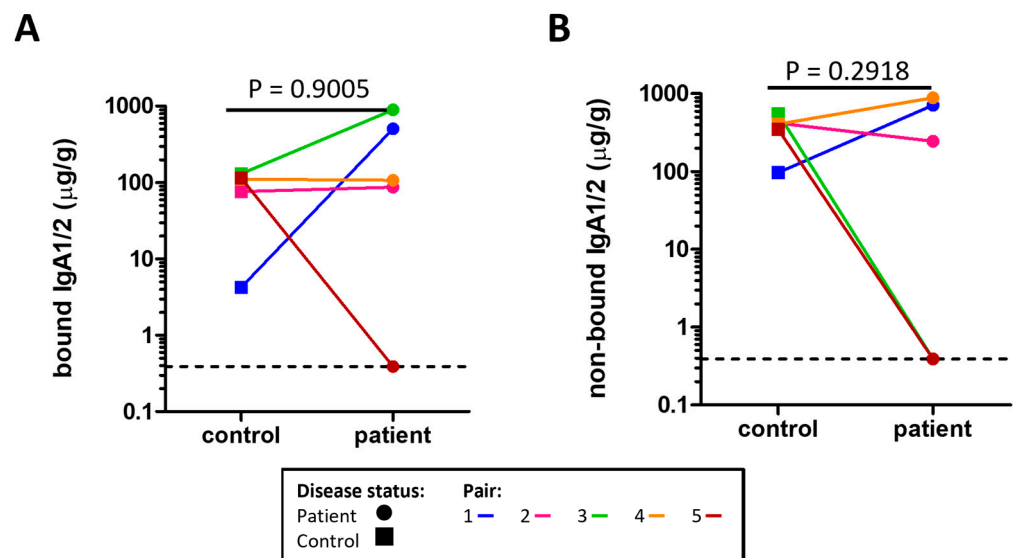


Figure 1. Concentration of sIgA measured by ELISA in the stool of severe ME/CFS patients ($n = 5$) and matched household controls ($n = 5$) for: (A) microbe bound sIgA; (B) microbe non-bound sIgA. For both plots, p values were calculated using a two-tailed paired t -test, the lowest value is identified by the dotted line.

2.5. Severe ME/CFS Patients Have a Reduced Serum IgG Immune Response to Stool Microbes

To determine whether immune tolerance to intestinal microbes was altered in severe ME/CFS patients the level of serum IgG antibodies bound to both their own (autologous) stool microbes and to non-self (heterologous) stool microbes from other individuals were measured in patients and their matched household controls (Figure 3A). Compared to their matched household controls, four patients had lower serum IgG reactivity to autologous stool microbes ($p = 0.07322$) (Figure 3B). In comparing serum IgG reactivity to heterologous microbes, all patients had lower serum IgG reactivity to heterologous microbes compared to that of their matched household controls' ($p = 0.006334$) (Figure 3C). Furthermore, controls had higher serum IgG reactivity to heterologous (their matched patient) stool microbes than to autologous stool microbes ($p = 0.0317$) (Figure 3D). In contrast, for patients there was no evidence for any differences in serum IgG reactivity to autologous and heterologous (their matched control) stool microbes ($p = 0.3619$) (Figure 3E). In addition, control individuals had higher serum IgG reactivity to patients stool microbes when compared to patients' serum IgG reactivity to their own stool microbes ($p = 0.003751$) (Figure 3F). Of note, the

reduced levels in patient IgG antibodies to autologous and heterologous stool microbes were not due to lower levels of serum IgG in patients (Figure 3G).

2.6. The Proportion of Microbes Bound by Serum IgG Is High in Both Patients and Controls

We next sought to determine how much of the stool microbiome was recognised by serum IgG by measuring the proportion of indigenous stool microbes coated by serum IgG (Figure 4A,B). There was no evidence for any differences in the proportion of stool microbes coated by IgG ('IgG positive') in severe ME/CFS patients compared with controls (Figure 4C). In determining the proportion of microbes bound by faecal IgG (Figure S4) only two severe ME/CFS patients and two controls had detectable faecal IgG.

When comparing the proportion of microbes bound by serum IgG to the proportion of microbes bound by faecal IgA, there was a small but insignificant positive correlation ($r(8) = 0.59$, $p = 0.802$).

2.7. Characterising the Stool Microbiome

Using whole metagenome shotgun sequencing, the microbial composition of SYBR Green+ ('all') stool microbes isolated by fluorescent activated cell sorting (FACS) was determined (Figure S5). The average number of 'all' microbes collected by FACS was 1.47 million. Taxa with a relative abundance greater than 1×10^{-6} were included in downstream analyses and comparisons made at the genus and species level.

At the genus level 275 taxa were detected. The 15 most abundant genera across all ME/CFS and matched household control samples ($n = 10$) were *Bacteroides* (10.4%), *Phocaeicola* (10.1%), *Clostridioides* (9.5%), *Lysobacter* (9.4%), *Faecalibacterium* (8.6%), *Blautia* (7.1%), *Roseburia* (5.8%), *Anaerostipes* (5.5%), *Akkermansia* (4.4%), *Campylobacter* (2.9%), *Agrobacterium* (2.6%), *Methanobrevibacter* (1.9%), *Bifidobacterium* (1.9%), *Anaerobutyricum* (1.5%) and *Streptococcus* (1.3%) (Figure S5A).

At the species level 705 taxa were detected. The 15 most abundant species across all ME/CFS and matched household control samples ($n = 10$) were *Clostridioides difficile* (9.5%), *Lysobacter enzymogenes* (9.4%), *Faecalibacterium prausnitzii* (8.6%), *Phocaeicola dorei* (6.4%), *Blautia* sp. SC05B48 (6.3%), *Anaerostipes hadrus* (5.4%), *Roseburia intestinalis* (4.5%), *Akkermansia muciniphila* (4.3%), *Bacteroides uniformis* (3.7%), *Phocaeicola vulgatus* (3.6%), *Agrobacterium tumefaciens* (2.5%), *Methanobrevibacter smithii* (1.8%), *Bacteroides cellulosilyticus* (1.6%), *Anaerobutyricum hallii* (1.5%) and *Campylobacter jejuni* (1.5%) (Figure S5C).

Using three measures of intra-sample diversity, the Shannon index, inverse Simpson index and observed richness, there was no evidence for differences in any of the alpha diversity measures between severe ME/CFS patients and matched household controls at the species level (Figure S6A).

Due to the large variation in microbial load in stool samples from severe ME/CFS patients (6.3×10^{10} cells/gram to 2.6×10^{11} cells/gram) and controls (1.2×10^{11} cells/gram to 2.0×10^{11} cells/gram) (Figure S3), converting relative abundances to absolute abundances increased the heterogeneity amongst samples at both the genus and species levels (Figure S5B,D). However, analysis of beta diversity using Bray–Curtis dissimilarity identified subtle changes in both relative microbiome profiles (RMP) and quantitative microbiome profiles (QMP). Samples from patients in pairs three, four and five were most dissimilar to the other samples whilst samples from patients in pairs one and two clustered together with their matched household controls (Figure S6B).

Functional differences in the microbiome of patients and controls were determined by comparing the abundance of gene families in the 'all' fraction. A total of 464,263 gene families were detected in all participants above the threshold. A further filtering step removed gene families below the threshold in more than seven samples, leaving 84,888 gene families for evaluation. Principal component analysis (PCA) was used to reduce the number of variables by defining principal components (PC) that highlighted the largest sources of variation amongst the samples. PC4 identified 11% of variation in functional genes families amongst samples that were attributable to disease status (Figure S7).

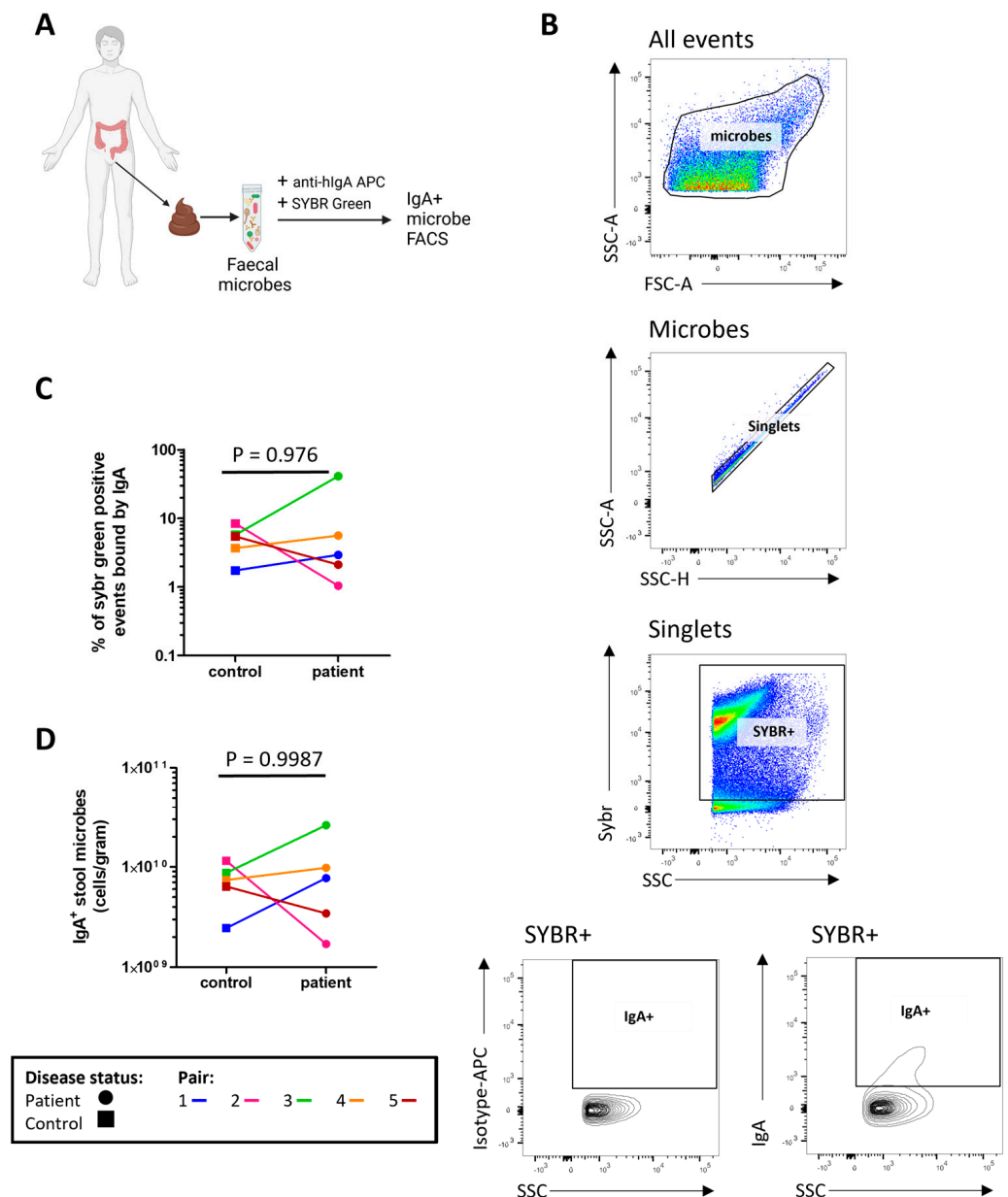


Figure 2. Profiling stool sIgA: (A) overview of sample preparation for sIgA-bound microbe fluorescent activated cell sorting (FACS) analysis; (B) representative flow cytometric analysis of sIgA-bound stool microbes; (C) proportion of stool microbes bound by sIgA in severe ME/CFS patients (n = 5) and matched household controls (n = 5); (D) analysis of sIgA-bound microbial load in severe ME/CFS patients (n = 5) and matched household controls (n = 5). *p* values were calculated using a two-tailed paired *t*-test.

2.8. IgG-Seq Identifies Antimicrobial Signatures Unique to Each Participant

Next, IgG-Seq was used to characterise the indigenous GI microbes bound by serum IgG in severe ME/CFS patients and matched household controls. Briefly, 'IgG positive' and 'IgG negative' microbes were isolated by FACS from bulk stool samples and processed for shotgun metagenomic sequencing to identify taxa preferentially bound by serum IgG (Figure 5A,B). The mean number of 'IgG positive' microbes collected by FACS was 1.05×10^6 . The mean number of 'IgG negative' microbes isolated by FACS was 1.30×10^6 . Taxa with a relative abundance greater than 1×10^{-5} in the 'all' fraction were included in the 'IgG positive' and 'IgG negative' fractions for downstream analyses. Taxonomic comparisons were made at the species level.

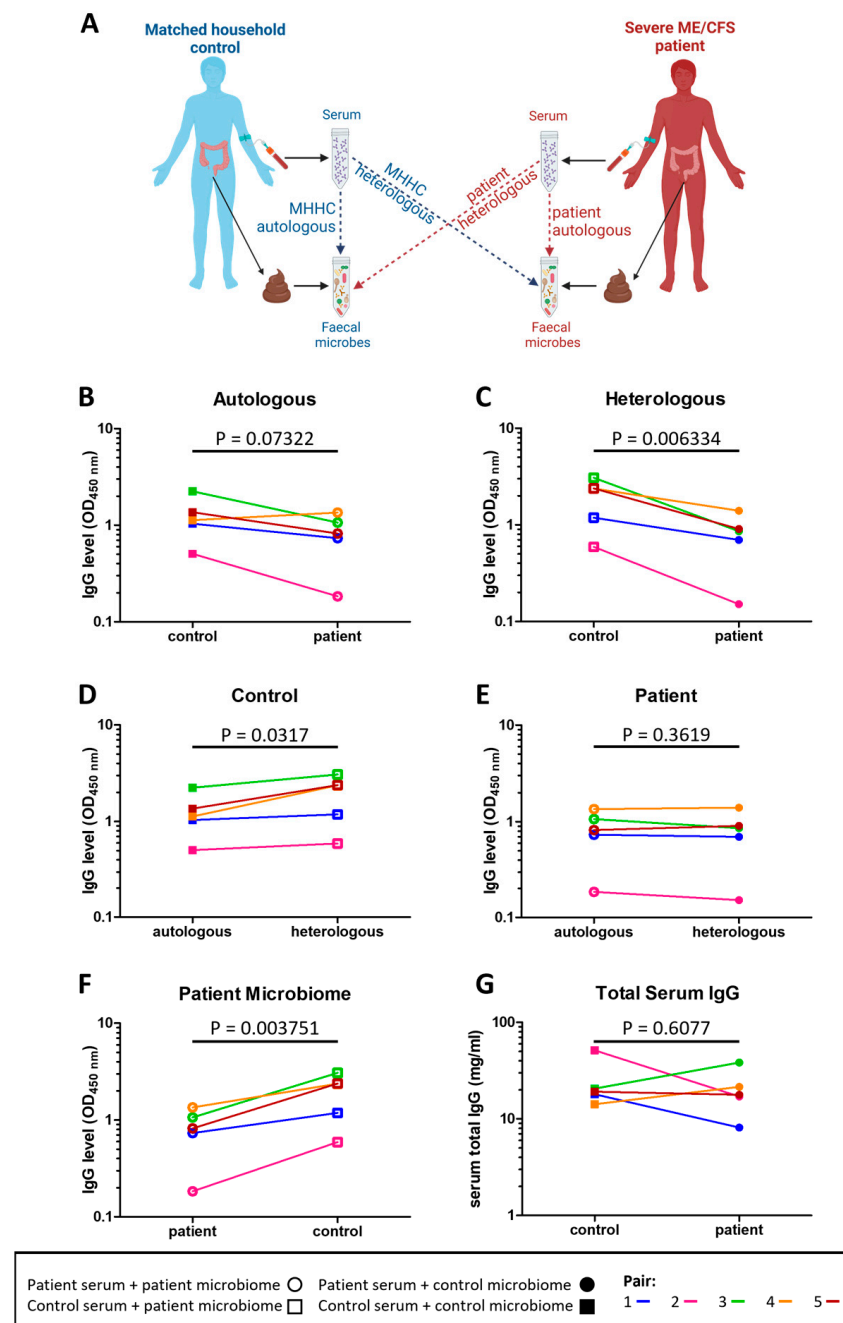


Figure 3. Serum IgG reactivity to autologous and heterologous stool microbes: (A) overview of assessment of IgG responses to indigenous (autologous) and foreign (heterologous) stool microbes in severe ME/CFS patients and matched healthy-household controls; (B) level of severe ME/CFS patient (n = 5) serum IgG and level of their matched household control (n = 5) serum IgG binding to autologous stool microbes in vitro; (C) level of severe ME/CFS patient (n = 5) serum IgG and level of their matched household control (n = 5) serum IgG binding to heterologous stool microbes in vitro; (D) level of household control (n = 5) serum IgG binding to autologous and heterologous stool microbes in vitro; (E) level of severe ME/CFS patient (n = 5) serum IgG binding to autologous and heterologous stool microbes in vitro; (F) level of household control (n = 5) serum IgG and severe ME/CFS (n = 5) serum IgG binding to stool microbes from the patient microbiome; (G) levels of IgG measured by means of ELISA in serum of severe ME/CFS patients (n = 5) and their matched household controls (n = 5). Two-tailed paired *t*-tests were used to calculate *p* values.

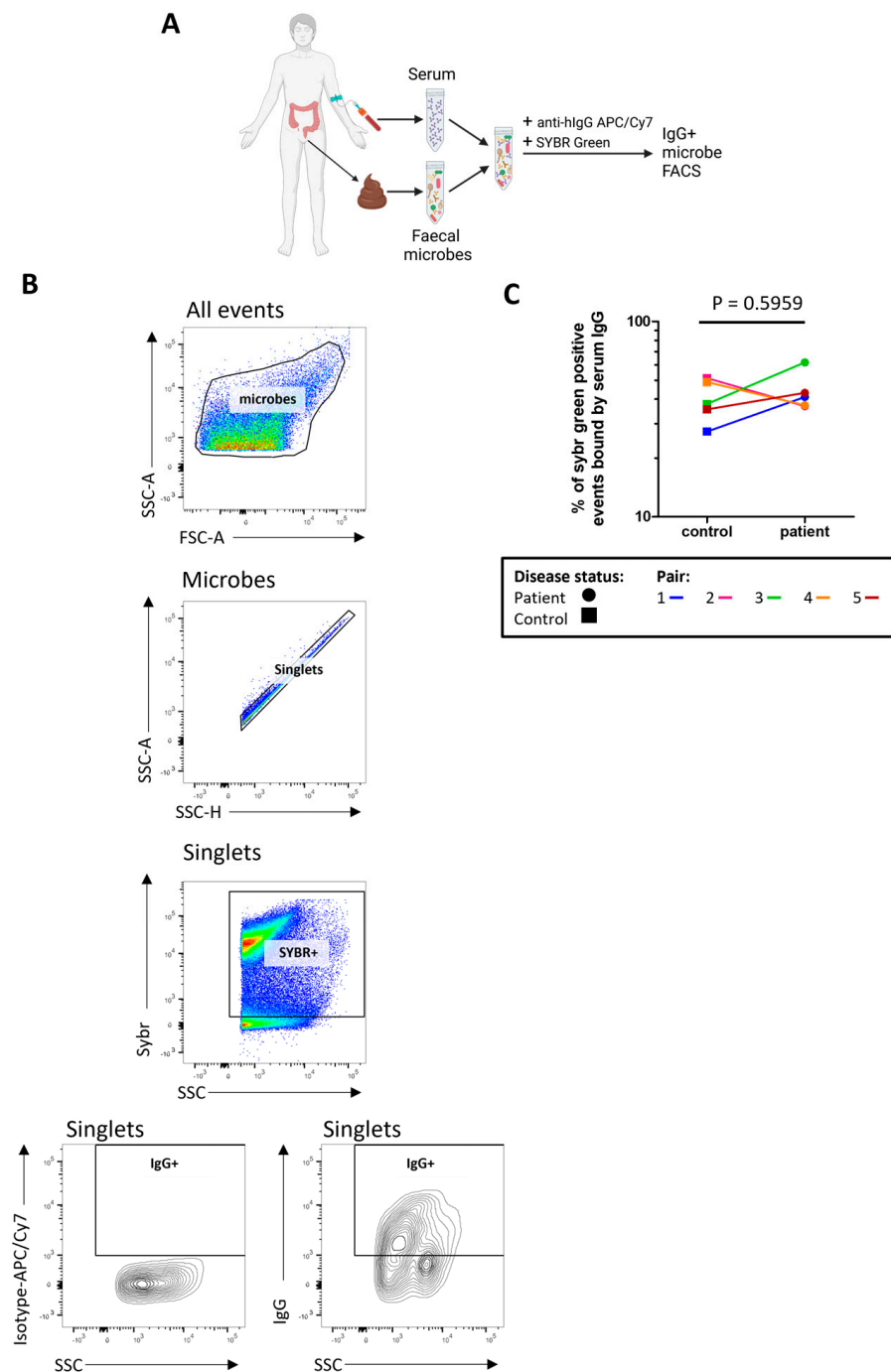


Figure 4. Quantifying stool microbes recognised by autologous serum IgG: (A) overview of sample preparation for IgG-bound microbe FACS analysis; (B) representative analysis of serum IgG binding to stool microbes, SYBR+ and IgG+ gates were defined using FMO controls and isotype controls were used to normalise IgG+ SYBR+ stool microbe readings; (C) analysis of the proportion of stool microbes bound by serum IgG in severe ME/CFS patients (n = 5) and matched household controls (n = 5). *p* values were calculated using a two-tailed paired *t*-test.

Observed richness scores were applied to rarefied reads to determine the number of microbial species with serum IgG reactivity (Figure 5C). All participants had more than 200 species in the ‘IgG positive’ fraction with a high number of species also identified in the ‘IgG negative’ fraction. Both patients and controls had a higher mean number of species in their ‘IgG negative’ fraction than their ‘IgG positive’ fraction (365 vs. 339 in patients and 358 vs. 322 in controls). However, most participants had a small number of species (<30)

exclusively in the 'IgG negative' fraction at a relative abundance $> 1 \times 10^{-5}$, except for the patient from pair three who had 107 species exclusively in their 'IgG negative' fraction (Table 2). In addition, this patient also had a smaller proportion of species recognised by IgG compared with all other participants (Table 2).

Table 2. Proportion of species detected that are recognised by serum IgG.

Pair	Participant	Number of Species Detected per Fraction			Proportion of Species IgG+
		Only IgG−	Only IgG+	Both IgG− and IgG+	
1	Patient	7	7	201	0.967
	Control	23	7	173	0.887
2	Patient	18	7	190	0.916
	Control	21	6	202	0.908
3	Patient	107	4	154	0.596
	Control	14	12	145	0.918
4	Patient	4	19	138	0.975
	Control	29	6	168	0.857
5	Patient	9	18	162	0.952
	Control	15	31	206	0.940

Next, we assessed the similarity/difference between 'IgG positive' and 'IgG negative' fractions in patients and controls using the Bray–Curtis index and visualising distances using an NMDS plot (Figure 5D). 'IgG positive' and 'IgG negative' fractions from the same participant shared the greatest similarity. No clustering was seen for either fraction in patients or controls. The 'IgG positive' and 'IgG negative' fractions from patients in pairs three and five were most dissimilar to the other samples.

Using the probability ratio developed by Jackson et al. (2021) [31], we scored IgG binding by directly measuring the likelihood of a species being bound by IgG. Positive IgG probability ratios indicate that a species is more likely to be coated with IgG and reside in the 'IgG positive' fraction. Conversely, negative IgG probability ratios indicate that a species is more likely to be uncoated and reside in the 'IgG negative' fraction. Probability ratios are not influenced by the relative abundance of a species within the 'all' fraction and therefore measure the quantity of IgG produced against a given species. Of the 423 species detected at a relative abundance greater than 10^{-5} , 101 species were detected in every participant and, therefore, used in downstream analysis. It is worth noting that despite detecting species falling into the bacteria, fungi, archaea and virus kingdoms, only bacterial species were detected in every participant and consequently used in downstream analysis. Notably, owing to the way in which probability ratios are calculated they tend to be similar across species within participants, with some having consistently lower estimates across all species than others, driven by their overall IgG probability ratio. Probability ratio scores varied amongst species and participants. Each participant had a unique combination of probability ratio scores for different species (Figure 6). We were unable to meaningfully test for differences in probability ratio scores between patients and controls for individual species due to the small sample size and lack of power to detect significant changes.

Finally, we analysed the function of the microbial communities within the 'IgG positive' and 'IgG negative' fractions by analysing the likelihood of a gene family being present in a microbe bound by IgG. IgG probability ratios were calculated for the 1724 gene families that were detected in all participants above the threshold. Using a PCA plot to assess how the ten samples varied with regards to the likelihood of certain gene families being present in microbes bound by IgG (Figure S8), a separation between severe ME/CFS patients and controls from four households was observed (PC2), corresponding to 13% of explained variance.

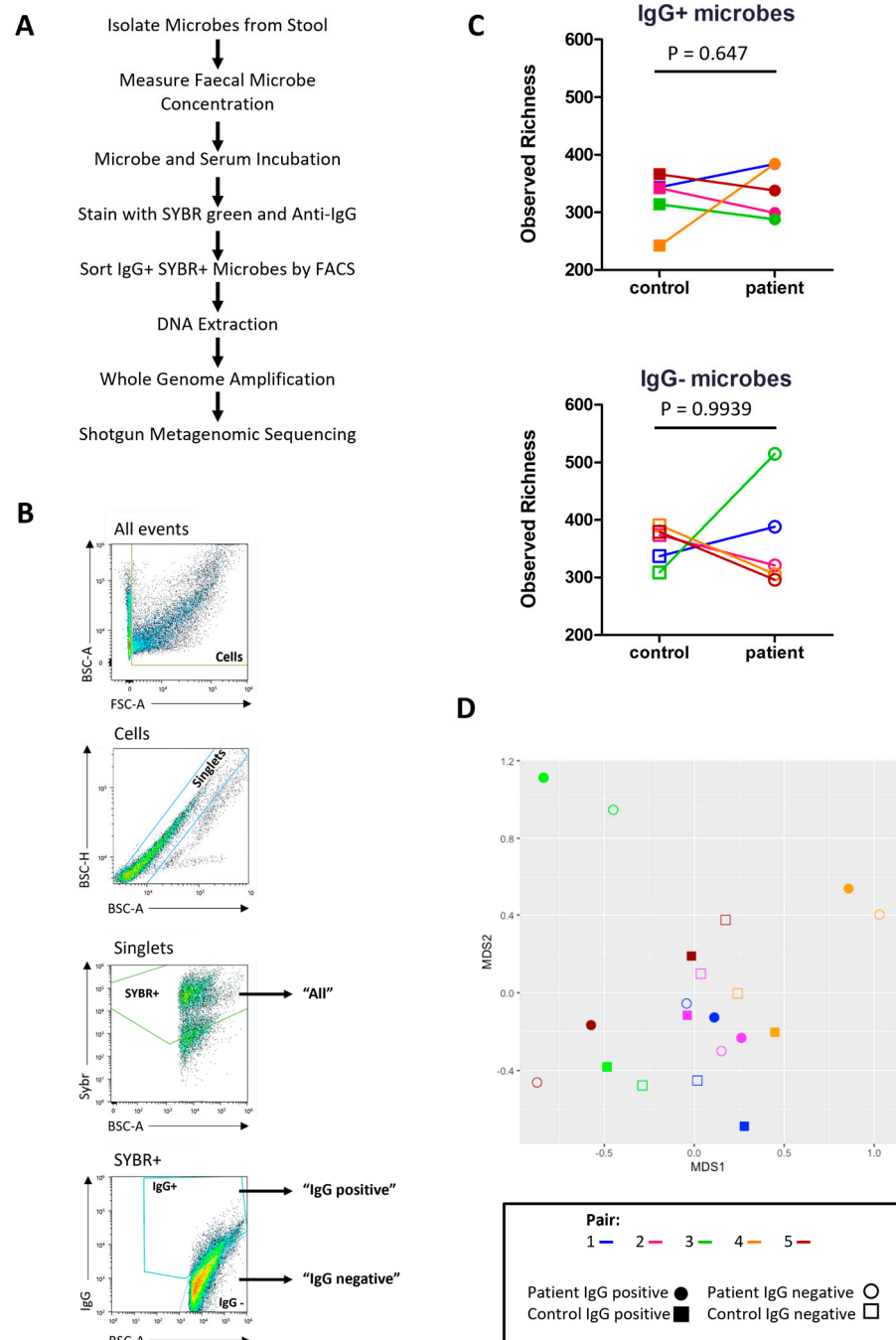


Figure 5. IgG-Seq: (A) IgG-Seq protocol used to determine taxa from stool samples reactive to autologous serum IgG; (B) representative flow cytometric dot plot showing IgG-Seq gating strategy based upon forward scatter (FSC) and back scatter (BSC) characteristics, followed by discrimination of singlets from doublets, SYBR+ microbes were discriminated from auto fluorescent debris and collected for profiling of all stool microbes, IgG positive and IgG negative populations were sorted from SYBR+ events; (C) pairwise comparisons of observed richness of IgG positive and IgG negative microbes in severe ME/CFS patients (n = 5) and matched household controls (n = 5), analyses were performed at the species-level, with reads rarefied to the lowest sequencing depth; (D) beta diversity of IgG positive species (filled shapes) and IgG negative species (unfilled shapes) in severe ME/CFS patients (circles) and household controls (squares). *p* values were measured using two-tailed paired *t*-tests. Beta-diversity was calculated using Bray–Curtis dissimilarity presented on a non-metric multi-dimensional scaling (NMDS) plot.

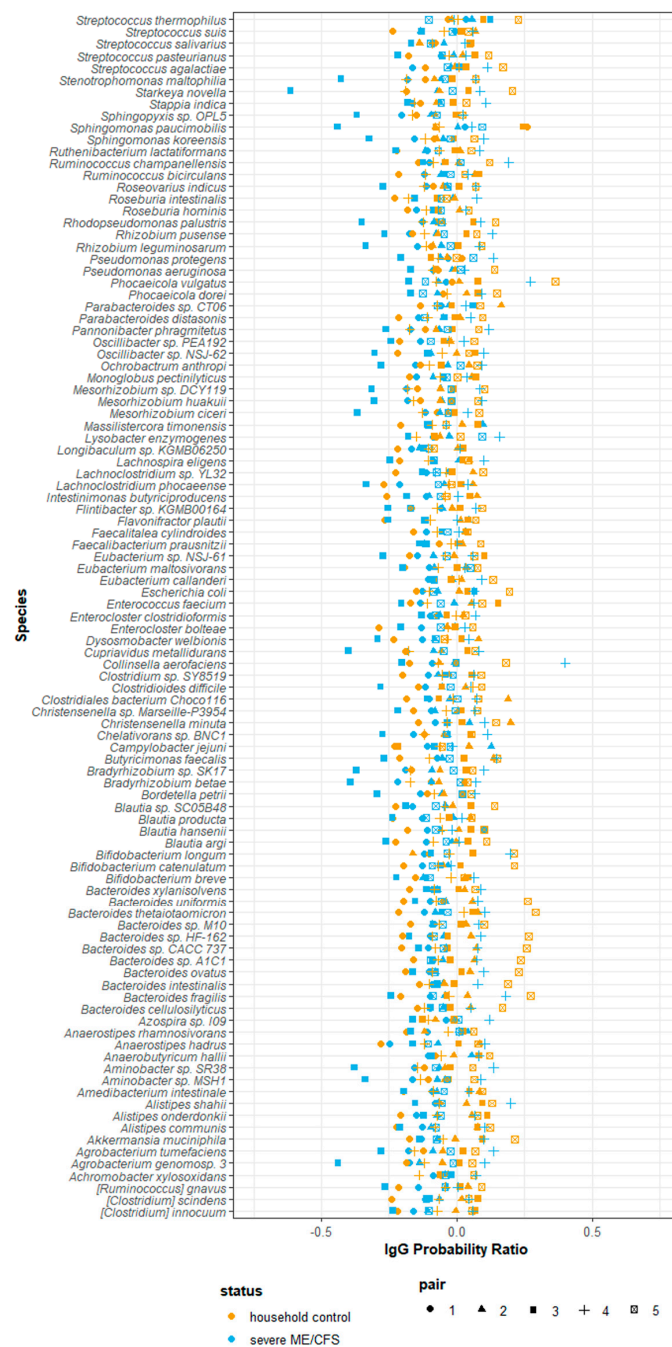


Figure 6. Probability of serum IgG binding to autologous stool microbes from severe ME/CFS patients (n = 5) and matched household controls (n = 5). IgG probability ratios for species detected in all participants stool samples.

3. Discussion

This pilot study highlights the logistical challenges of including severe, house- or bedbound ME/CFS patients in research studies and collecting biological samples. Contrary to our initial hypothesis, our findings from a small cohort of patients and controls suggests that severe ME/CFS patients may have a reduced serum IgG immune response to stool microbes.

3.1. Lessons Learnt for the Inclusion of Severe ME/CFS Patients in Biomedical Research

Despite their significant disability severe ME/CFS, patients were enthusiastic and eager to participate in our study with a 58% response rate. However, severe ME/CFS often

coincided with additional illness complications that excluded these individuals from the study, hindering recruitment. We also found that symptom severity of house or bedbound ME/CFS patients fluctuated, making it difficult to arrange home study visits. The wide geographical distribution of participants' homes (30–140 miles from the research institute) restricted sample collection with a minimum of 2 h required for sample collection and transportation to the laboratory. Therefore, a multi-centre effort is needed to reduce the size of the geographical location served by one research institute.

We recruited controls from the same household as the patient to account for environmental confounders of microbiome analyses such as living conditions and diet [32,33]. Previous studies have shown that inclusion of same-household controls enables identification of ME/CFS disease-specific microbiome changes [34]. However, the requirement for a matched healthy-household control impacted on patient recruitment. Amongst patients not meeting the study eligibility criteria, 44% were excluded due to being unable to identify a matched household control. Considering that household controls were typically carers and parents or spouses of the patient, it was not possible to match age and gender of patients and controls, both of which are confounding variables for immunological [35,36] and microbiome studies [37]. Other confounders potentially discordant amongst patients and controls were BMI, exercise and medications. Our finding of a sparse clustering between results from severe ME/CFS patients and matched household controls suggests that these and perhaps other confounding variables had an influence on immune response to the intestinal microbiome. To enhance research participation of severe ME/CFS patients, future studies should consider recruiting age-, gender- and BMI- matched sedentary controls.

3.2. Severe ME/CFS Patients Have Serum IgG Hyporeactivity to Stool Microbes

The hypothesis guiding our study was that ME/CFS patients have increased intestinal permeability due to an altered microbiome, which results in translocation of intestinal microbes into the circulation, triggering an immune response. Despite the low study sample size, we found evidence that severe ME/CFS patients in fact have lower serum IgG levels reactive to stool microbes than their matched household controls. This appears to be a property of the patients' immune responses, rather than their microbiome which structurally and functionally closely resembled that of their matched controls. Our findings mirror the findings from pioneering studies investigating immune reactivity to faecal microbes in IBD patients which demonstrated that healthy controls have higher serum IgG reactive to heterologous stool microbes than to autologous stool microbes [15]. In our study, heterologous reactivity was measured using samples from individuals living in the same household which are known to display greater similarity to patients' microbiomes than individuals living in different households [38]. This should increase confidence in identifying microbes that distinguish the microbiome of patients from controls as being a property of the disease. Despite this advantage, there were no differences in alpha diversity measures between severe ME/CFS patients and matched household controls at the genus or species level. Instead, our findings provide initial evidence for immune dysfunction in ME patients manifesting as a reduced capacity and reactivity of serum IgG to stool microbes irrespective of their source. Previous studies have described IgG immunodeficiencies in ME [39] which could explain why we found reduced levels of serum IgG binding to stool microbes in severe ME/CFS patients. However, there was no evidence of IgG immunodeficiencies in our severe ME/CFS patient cohort. Instead, it may be attributable to IgG antibody repertoires and a less diverse repertoire of antibodies directed at intestinal microbes. The loss of antibody diversity occurs naturally during ageing and is a defining feature of immune senescence and declining immune function in later life [40]. The possibility of premature or accelerated immunosenescence should be a focus of future studies, particularly as it relates to effector immune cells whose functionality is compromised in ME patients, as previously described for NK cells [41], and here for B cells. An additional possibility relates to immune hibernation in ME/CFS patients which

produces a hypometabolic state [42] that may limit lymphocyte responsiveness to foreign antigens and increased tolerance to bacterial endotoxins [43].

3.3. Limitations of this Pilot Study in Addressing the Study Hypothesis

The severe ME/CFS patients recruited to this pilot study had comorbid IBS, whereas household controls were free of any GI complaints. IBS comorbidity is a confounding variable in ME/CFS microbiome studies as defined microbiome profiles have been described that discriminate between patients with and without IBS comorbidity [9]. To establish whether the results found in this pilot study of severe ME patients are disease specific future studies should compare severe ME/CFS patients with and without comorbid IBS and compare severe ME/CFS patients with comorbid IBS to IBS patients.

The presence of increased intestinal permeability within the severe ME/CFS patient cohort was not investigated in the present study. Based upon previous studies, a majority of ME patients (~67%) have increased intestinal permeability compared with healthy controls [13]. An intact intestinal barrier in the severe ME/CFS patients recruited to this study might explain why they did not have increased IgG reactivity to autologous stool bacteria compared with their matched healthy-household controls. It has been shown that levels of IgG reactive to autologous stool bacteria are elevated in other diseases associated with increased intestinal permeability such as Crohn's disease [16]. Future studies should seek to establish the integrity of the intestinal barrier in severe ME/CFS patients.

The present study only assesses serum IgG reactivity to autologous stool microbes at a single time point which may not account for the dynamic microbiome and compositional shifts over time [44]. In addition, IgG reactivity to microbes that are absent from stool at the time of sampling could not be assessed. Longitudinal studies would address these issues and the impact of microbiome changes on serum IgG reactivity over time. An alternative approach is to create a surrogate faecal community [30], pooled from multiple donors, although this would mask individual variations.

The IgG-Seq protocol used in this research identified serum IgG produced in response to bacteria and fungi. Whilst excluding reactivity to other constituents of the intestinal microbiome in the current study, the method can be adapted to detect IgG reactivity to viruses and archaea that can then be identified and isolated using FACS.

3.4. Conclusions

Severe ME patients have historically been excluded from research studies. This pilot study demonstrates the feasibility and challenges associated with including this important and growing population of ME patients in research. In providing evidence of immune dysfunction in severe ME/CFS patients, expressed as hyporesponsive serum IgG responses to intestinal microbes, this study also provides the theoretical and methodological basis and rationale for undertaking more detailed immune function studies in larger cohorts of ME patients.

4. Materials and Methods

4.1. Participant Recruitment

Ten volunteers were enrolled onto this study between 2018 and 2019: five severe ME/CFS patients and, as controls, five healthy individuals that were the patients' carers and living in the same household. Severe ME/CFS participants were recruited by the tertiary referral centres ESTH CFS Service, Carshalton, UK, and the ECCHC ME/CFS service, Lowestoft, UK. All severe ME/CFS patients had a confirmed diagnosis of ME/CFS based on a hybrid of the NICE 2007 guidelines [45] and the CDC-1994 criteria [46] and defined as experiencing at least four of the following symptoms for a minimum of 4 months; cognitive difficulties, muscle pain, multi-joint pain, new headaches, recurrent sore throats, cervical/axillary lymphadenopathy, unrefreshing sleep and post-exertional malaise. Severity was based on being unable to undertake activities associated with daily living, wheelchair dependency for mobility and being house or bedbound and requiring aid for washing,

using the toilet and eating. All patients were asked to complete the Chalder fatigue questionnaire, shortened medical outcomes study, 36-item short-form health survey (SF-36), hospital anxiety and depression scale (HADS), a self-efficacy questionnaire, visual analogue pain rating scale and the Epworth sleepiness scale. Matched household controls were defined as individuals who were living with or caring for the severe ME/CFS patient. Matched household controls were excluded if they had a long-term medical condition, in particular GI conditions, autoimmune diseases, anxiety, or depression, or were receiving immunomodulatory drugs, statins, beta blockers or steroids. Participants consuming antibiotics or probiotic capsules within the 6 weeks prior to sample collection were excluded.

The study was performed in accordance with the Declaration of Helsinki and the International Conference on Harmonisation Good Clinical Practice (ICH GCP) Guideline, and in compliance with national law. The research was approved by the NHS Health Research Authority London Hampstead Research Ethics Committee (REC 17/LO/1102, IRAS ID 218545). This study was registered on the clinicaltrials.gov database (NCT03254823). All participants provided fully informed written consent. The collection, storage and use of human tissue samples was carried out within the terms of the Human Tissue Act 2004 (Human Tissue Authority).

4.2. Sample Collection and Processing

Fresh stool and blood samples were collected from each participant within a 24 h window during a home visit. Twenty millilitres of blood was collected in BD Vacutainer[®] serum separator tubes (BD Biosciences, Wokingham, UK). Serum was separated from whole blood following the manufacturers protocol and immediately stored at -80°C . Stool samples were collected immediately after defecation in a Fecotainer[®] (AT Medical BV, Enschede, The Netherlands) with an Oxoid[™] AnaeroGen[™] compact sachet (Thermo Scientific, Hemel, UK) to preserve anaerobic bacteria. The consistency and appearance of fresh stool samples was recorded using the BSFS [47]. Stool samples were stored at 4°C for <24 h. Following homogenisation, aliquots of the bulk homogenate and of 40% stool microbial glycerol suspensions were stored at -80°C . Glycerol stocks were prepared by diluting stool samples (10% *w/v*) with PBS, collecting the supernatant following centrifugation at $300\times g$ for 5 min at 20°C and diluted 1:1 with 80% *v/v* glycerol.

4.3. Stool Water Content

Non-diluted aliquots of stool were weighed before and after freeze drying using the ModulyoD freeze dryer (Richmond Scientific Limited, Chorley, UK) for 12 h. Water content was calculated using the following equation.

$$\frac{(\text{wet weight} - \text{dry weight})}{\text{wet weight}} \times 100, \quad (1)$$

4.4. Stool Microbial Load

Non-diluted stool aliquots were thawed on ice and diluted (1% *w/v*) with PBS solution containing 0.1% *w/v* BSA fraction V. Samples were homogenised using a Kimble[™] Kontes[™] Pellet Pestle[™] Cordless motor (Sigma-Aldrich, Saint Louis, MO, USA) and filtered through a $70\ \mu\text{m}$ cell strainer. Filtered microbial suspensions were diluted 1:1600, 1:3200 and 1:6400; then, 200 μL of each dilution were incubated with 10 μL of 1:100 SYBR[™] Green I nucleic acid gel stain (ThermoFischer Scientific, Paisley, UK) for 30 min. Microbial load was determined using the Guava[®] easyCyte[™] 5HT equipped with a 488 nm laser (Luminex Corporation, Austin, TX, USA). Prior to sample acquisition the instrument was cleaned following manufacturers' instructions and calibrated using the Guava[®] easyCheck[™] kit. Stool microbes (SYBR Green+ events) were enumerated using Guava[®] Suite Software v3.3.

4.5. Stool IgA Concentration

Non-diluted stool aliquots were thawed on ice, diluted (10% *w/v*) with 0.2 M NaHCO₃, pH 9.4 and homogenised using a Kimble™ Kontes™ Pellet Pestle™ Cordless motor. Samples were centrifuged twice at 16,000× *g* for 5 min at 20 °C and after both rounds of centrifugation the pellet and supernatant were separated. The supernatants were pooled and used to analyse free sIgA by ELISA. The pellet was washed and resuspended to the original volume using 0.2 M NaHCO₃, pH 9.4, and used to analyse microbe associated/bound sIgA by ELISA. All reactants except for the blocking solution and wash buffers were added in volumes of 100 µL/well. All washes were repeated three times with PBS and 0.05% Tween™ 20 unless otherwise stated. Nunc MaxiSorp™ flat-bottom plates (Thermo Fisher Scientific) were coated for 16 h at 4 °C with 10-fold serial dilutions (1 to 1:1,000,000) of samples and with twofold serial dilutions (250–3.9 ng/mL) of a human colostrum IgA standard (Sigma-Aldrich), diluted with 0.2 M NaHCO₃, pH 9.4. Samples and standards were plated in duplicate. Plates were washed and then blocked for 3 h with 300µL/well of PBS, 0.05% Tween™ 20, 2% BSA fraction V, 1% normal mouse serum (Thermo Fisher Scientific). Plates were washed and then incubated with 1000 ng/mL BD Pharmingen™ biotin conjugated mouse anti-human IgA1/IgA2 monoclonal antibody (clone G20-359, BD Biosciences) diluted in PBS, 0.05% Tween™ 20, 2% BSA fraction V, 1% normal mouse serum. After 1 h of incubation at 20 °C plates were washed and incubated with 1:80,000 HRP-Conjugated Streptavidin (Thermo Fisher Scientific) diluted in PBS, 0.05% Tween™ 20, 2% BSA fraction V, 1% normal mouse serum for 30 min at 20 °C. Plates were washed six times and incubated with TMB high sensitivity substrate solution (BioLegend® UK Ltd., London, UK) for 5 min. The addition of 2N H₂SO₄ stopped the reaction and absorbances were read at 450 nm. IgA sample values were determined by reference to standard curves.

4.6. Serum IgG Quantification

Total serum IgG was measured using the commercial Invitrogen IgG (Total) Human Uncoated ELISA kit (Thermo Fisher Scientific). Samples were measured in duplicate.

4.7. Serum IgG Levels to Autologous and Heterologous Stool Microbes

Glycerol stocks of stool microbes were thawed and washed three times with PBS at 8000 *g* for 5 min at 20 °C. The pellet was resuspended in 1 mL PBS. Serial dilutions (twofold) of stool microbes in PBS were plated in duplicate in a 96-well flat bottom Corning™ Costar™ 9018 plate. Absorbances were read at 570 nm and stool microbes were resuspended to an optical density of 0.05 with 0.1 M NaHCO₃, pH 9.4.

Serum IgG reactivity to autologous ('self') or heterologous ('non-self', matched patient or control) stool microbes was measured by ELISA. All washes were repeated three times with 200 µL/well PBS and 0.1% Tween™ 20 unless otherwise stated. Nunc MaxiSorp™ flat-bottom plates (Thermo Fisher Scientific) were coated for 16 h at 4 °C with 100 µL/well of stool microbes. Plates were washed and then blocked for 3 h at room temperature under agitation with PBS, 2% BSA fraction V, 1% normal goat serum (Sigma-Aldrich). Plates were incubated for 1 h at 20 °C with 50 µL/well of complement inactivated serum samples diluted 1:160 in PBS, 2% BSA fraction V, 1% normal goat serum. Plates were washed and incubated for 1 h at room temperature under agitation with 100 µL/well of 1:500 goat anti-human IgG H&L (HRP) (ab81202, Abcam, Cambridge, UK), diluted in PBS, 2% BSA fraction V, 1% normal goat serum. Plates were washed six times and incubated with TMB high sensitivity substrate solution (BioLegend® UK Ltd.) for 5 min at 20 °C. The addition of 0.16 M H₂SO₄ stopped the reaction and absorbances were read at 450 nm. Results were normalised by subtracting serum only absorbance readings from sample readings.

4.8. Microbial Flow Cytometry

Systemic and faecal IgG and faecal IgA binding to stool microbes was assessed by microbial flow cytometry. All buffers were filter sterilised using a 0.22 µm filter before use. Aliquots of non-diluted stool samples were processed and the microbial concentra-

tion in each stool sample measured as described earlier. Microbes were resuspended to 2×10^6 cells/mL in PBS with 0.1% BSA. 500 μ L of complement inactivated serum was diluted 1:100 in PBS with 0.1% BSA and incubated for 30 min at 20 °C with 200 μ L of 1×10^6 cells/mL of stool microbes. For secretory IgA and faecal IgG measurements stool microbes were not incubated with serum. Samples were washed in PBS with 0.1% BSA (5 min, 1.2×10^4 rpm) and microbes were resuspended to 1×10^6 cells/mL and incubated with 1:1000 SYBR™ Green I nucleic acid gel stain and 1:100 secondary conjugated antibodies anti-human IgA-APC (clone 1S11-8E10, Miltenyi Biotec, Bisley, UK) and anti-human IgG-APC/Cy7 (clone HO6017, BioLegend® UK Ltd.) or their respective isotype controls. Samples were fixed with 0.75% *v/v* paraformaldehyde. Acquisition of cellular events was performed using the BD LSRFortessa™ (BD Biosciences) and analysed using FlowJo™ software version 10.7.1. Gates were defined using fluorescence minus one (FMO) controls. Frequencies of antibody bound stool microbes were expressed as percentages. The percentage of Ig-bound microbes was normalised by subtracting frequency of Ig-bound microbes measured using isotype controls.

4.9. Metagenomic Shotgun Sequencing Analysis of Total Gut Microbiota and IgG-Coated Microbes (IgG-Seq)

4.9.1. Microbial Cell Sorting

Non-diluted stool samples were processed, incubated with serum and stained for IgG flow cytometry analysis as described previously. Isotype controls were not used in microbial cell sorting. Microbes were diluted to 1×10^7 cells/mL and cell sorting achieved using the Sony SH800S cell sorter equipped with four lasers: 488 nm, 405 nm, 638 nm and 651 nm (Sony Biotechnology, Weybridge, UK). Prior to sample acquisition the instrument was cleaned and calibrated according to the manufacturer's instructions and gates were defined using FMO controls. Microbes (1×10^6) were collected from the following three fractions: (1) 'all' (SYBR+ microbes), (2) 'IgG positive' (SYBR+IgG+), (3) 'IgG negative' (SYBR+IgG−). Fractions were centrifuged and immediately stored at −20 °C as dry pellets.

4.9.2. DNA Extraction, Processing and Sequencing

DNA was extracted using the Gram-positive bacteria genomic DNA purification protocol from the GeneJET DNA genomic DNA purification kit (Thermoscientific) with the following modifications: (1) 0.52 kU/mL achromopeptidase was added to the lysis buffer and the incubation time increased to 60 min; (2) incubation with lysis solution and proteinase K was increased to 50 min. DNA was precipitated using 0.7X solid phase reversible immobilisation bead clean-up with KAPA pure beads (Roche, Basel, Switzerland). Whole genome amplification was performed using the REPLI-g advanced DNA single cell kit (QIAGEN Ltd. Manchester, UK). The quality and quantity of amplified genomic DNA were determined using the 4200 TapeStation (Agilent, Stockport, UK) and the Quanti-iT™ dsDNA high sensitivity assay kit (Thermo Fisher Scientific). A ready-to-load pooled sequencing library was prepared by the in-house QIB sequencing service using the Illumina DNA prep kit (20018704, Illumina, Cambridge, UK) and the KAP2G Robust PCR kit (Sigma-Aldrich), followed by sequencing using 2×150 bp paired-end chemistry (PE150) on the Illumina NovaSeq 6000 platform (Novogene Ltd., Cambridge, UK).

Paired-end sequencing reads were provided as FASTQ format. All raw sequencing reads were pre-processed using tools retrieved from the BioConda repository [48]. SeqFu (v1.8.5) [49] was used to assess the quality of raw sequencing reads and those bases below Phred quality score of 15 were removed using Fastp (v0.20.0) [50]. Human genomic DNA identified by Kraken2 [51] against the Genome Reference Consortium Human Build 37 (GRCh37/hg19) database were removed. Taxonomic assignment of remaining sequencing reads was performed using Kraken2 [51] against the 'PlusPF' database containing archaea, bacteria, viral, plasma, human1, UniVec_Core, Protozoa and Fungi <https://benlangmead.github.io/aws-indexes/k2> (accessed on 4 January 2021). Abundance of reads at the species

level was estimated using Bracken [52]. Taxonomic read counts were converted to relative abundances by total sum scaling to 1.

4.9.3. Relative and Quantitative Microbiome Profiling

The ‘all’ fraction from microbial cell sorting was used for RMP and QMP. The cut off threshold of 1×10^{-6} was applied to relative abundances and a pseudocount of 1×10^{-7} was added. The microbial load of each species was calculated on these modified relative abundances using the equation below.

$$\text{absolute abundance (cells/g)}_{ij} = RA_{ij} \times \text{total cell concentration (cells/g)}_j \quad (2)$$

4.9.4. Analysing IgG Binding of Taxa

RMP data were used for IgG binding analysis with a cut off threshold of 1×10^{-5} . In addition, for each participant if a species was not detected in the ‘all’ fraction above the threshold then this species was subsequently removed from respective ‘IgG positive’ and ‘IgG negative’ fractions. The ‘IgAScores’ (v.0.1.2) [31] R package was used to calculate IgG probability ratios for taxon i in sample j using the ‘igascores’ function with method set to ‘probratio’, pseudocount ‘c’ set to 1×10^{-5} and ‘scaleratio’ set to TRUE. ‘IgG positive’ and ‘IgG negative’ fraction sizes are included in Table S1.

$$\text{probability ratio}_{ij} = \log_2 \left(\frac{\left(\text{IgG}_{ij}^+ \times \text{Fraction size}_j^{\text{IgG}^+} \right) + c}{\left(\text{IgG}_{ij}^- \times \text{Fraction size}_j^{\text{IgG}^-} \right) + c} \right) \quad (3)$$

4.9.5. Alpha Diversity

The diversity function from the ‘vegan’ R package (v.2.5-7) [53] was used to calculate Shannon indices and inverse Simpson indices. The rarefy function from ‘vegan’ (v.2.5-7) [53] was used to rarefy reads to the lowest sequencing depth. Observed species’ richness was the number of species remaining following rarefaction.

4.9.6. Beta Diversity

The vegdist function from ‘vegan’ (v.2.5-7) [53] was used to calculate Bray–Curtis indices on relative abundances. The metMDS function from ‘vegan’ (v.2.5-7) [53] was used to performed non-metric multidimensional scaling (NDMS) on Bray–Curtis indices.

4.9.7. Functional Analysis

Gene families were identified using the HMP Unified Metabolic Analysis Network 3.0 (HUMANn 3.0) package from the bioBakery suite [54,55]. In all participants each gene family was filtered by the following criteria: if a gene family was not present in the ‘all’ fraction the reads per kilobase (RPK) were zeroed in the ‘IgG positive’ and ‘IgG negative’ fractions of that participant. The humann_renorm_table utility script from HUMANn 3.0 was used to convert gene families from RPK to relative abundances. Community level classifications of gene families were used in downstream analysis. A cut off threshold of 1×10^{-6} was applied to all samples.

To analyse gene families in the microbiome of severe ME/CFS patients compared with household controls the ‘all’ fraction was used. Gene families that were below the threshold in seven or more samples were discarded from downstream analysis. The clr function from the ‘compositions’ R package (v 2.0-4) [56] was used to CLR transform the relative abundance of gene families. The pca function from the ‘mixOmics’ R package (v 6.18.1) [57] was used to perform PCA on gene families. Severe ME/CFS patients and their matched household controls were not treated as paired samples in this analysis.

To analyse gene families of IgG reactive microbes IgG, probability ratios were calculated using the relative abundance of gene families in the ‘IgG positive’ fraction and the ‘IgG negative’ fraction as described earlier, with a pseudocount set to 6×10^{-10} . Gene families

that did not have IgG probability ratios in all samples were discarded from downstream analysis. PCA was then performed as described previously.

4.10. Statistical Analysis

Statistical analyses and graphical representations were performed in R using the following packages: 'ggplot2' (v3.4.0) [58], 'reshape2' (v1.4.4) [59], 'data.table' (v1.14) [60], 'dplyr' (v1.1.0) [61], 'ggpubr' (V0.5.0) [62]. Graphs were also made using GraphPad Prism 5.04. Prior to analysis, data were log-transformed if there was evidence for non-normality. Pairwise comparisons between severe ME/CFS patients and their matched household controls were performed using a two-tailed paired *t*-test. Correlations were assessed with Pearson (*r*) correlation test.

4.11. Common Data Elements for ME Research

This study used the National Institute of Neurological Disorders and Stroke Common Data Elements guidelines' for reporting microbiome/microorganisms biomarkers in ME/CFS research (<http://www.commondataelements.ninds.nih.gov/>, accessed on 20 April 2023) [63].

Supplementary Materials: The following supporting information can be downloaded at: <https://www.mdpi.com/article/10.3390/ijms242015316/s1>.

Author Contributions: Conceptualization, K.A.S. and S.R.C.; methodology, K.A.S. and A.H.; formal analysis, K.A.S., A.T., S.K.T., M.D. and G.M.S.; investigation, K.A.S., A.L.S.d.C.-K., S.A.J. and A.N.; resources, A.B., S.R.C. and K.A.S.; data curation, A.T., K.A.S. and S.K.T.; writing—original draft preparation, K.A.S.; writing—review and editing, K.A.S., S.R.C. and T.W.; visualization, K.A.S., A.T., M.D., G.M.S. and S.K.T.; supervision, S.R.C. and T.W.; project administration, S.R.C. and K.A.S.; funding acquisition, S.R.C. All authors have read and agreed to the published version of the manuscript.

Funding: This research was joint funded by the UK charity Invest in ME Research (charity number 1153730) and the University of East Anglia (S.R.C.) with support from the Biological Sciences Research Council (BBSRC) Institute Strategic Programme Grant Gut Microbes and Health BB/R012490/1 and its constituent projects BBS/E/F/000PR10353, BBS/E/F/000PR10355 and BBS/E/F/000PR10356 (S.R.C.) and by the BBSRC Core Capability Grant BB/CCG1860/1 (G.M.S. and M.D.).

Institutional Review Board Statement: The study we performed in accordance with the Declaration of Helsinki and the International Conference on Harmonisation Good Clinical Practice (ICH GCP) Guideline, and in compliance with national law. The research was approved by the NHS Health Research Authority London Hampstead Research Ethics Committee (REC 17/LO/1102, IRAS ID 218545). This study was registered on the clinicaltrials.gov database (NCT0325423). All participants provided fully informed written consent. The collection, storage and use of human tissue samples was carried out within the terms of the Human Tissue Act 2004 (Human Tissue Authority).

Informed Consent Statement: Informed consent was obtained from all subjects involved in the study.

Data Availability Statement: The raw data are available at the European Nucleotide Archive under study accession number PRJEB1661 (<http://www.ebi.ac.uk/ena/browser/view?PRJEB1661>, accessed on 27 April 2023).

Acknowledgments: We acknowledge East Coast Community Health Care CFS Service and the CFS Clinic at Epsom and St Helier University Hospitals NHS Trust for help in recruiting patients, the QIB Human Research Governance Committee (HGRC) for reviewing the HRA ethics application and all the research participants who generously shared their time.

Conflicts of Interest: The authors declare no conflict of interest or competing interest. The funders played no role in the collection, analyses, or interpretation of data, in the writing of the manuscript, or in the decision to publish the results.

References

1. Lim, E.J.; Son, C.G. Review of case definitions for myalgic encephalomyelitis/chronic fatigue syndrome (ME/CFS). *J. Transl. Med.* **2020**, *18*, 289. [[CrossRef](#)] [[PubMed](#)]
2. Pendergrast, T.; Brown, A.; Sunnquist, M.; Jantke, R.; Newton, J.L.; Strand, E.B.; Jason, L.A. Housebound versus nonhousebound patients with myalgic encephalomyelitis and chronic fatigue syndrome. *Chronic Illn.* **2016**, *12*, 292–307. [[CrossRef](#)] [[PubMed](#)]
3. Chu, L.; Valencia, I.J.; Garvert, D.W.; Montoya, J.G. Onset Patterns and Course of Myalgic Encephalomyelitis/Chronic Fatigue Syndrome. *Front. Pediatr.* **2019**, *7*, 12. [[CrossRef](#)] [[PubMed](#)]
4. Lim, E.J.; Ahn, Y.C.; Jang, E.S.; Lee, S.W.; Lee, S.H.; Son, C.G. Systematic review and meta-analysis of the prevalence of chronic fatigue syndrome/myalgic encephalomyelitis (CFS/ME). *J. Transl. Med.* **2020**, *18*, 100. [[CrossRef](#)]
5. Salari, N.; Khodayari, Y.; Hosseinian-Far, A.; Zarei, H.; Rasoulpoor, S.; Akbari, H.; Mohammadi, M. Global prevalence of chronic fatigue syndrome among long COVID-19 patients: A systematic review and meta-analysis. *Biopsychosoc. Med.* **2022**, *16*, 21. [[CrossRef](#)] [[PubMed](#)]
6. Missailidis, D.; Annesley, S.J.; Fisher, P.R. Pathological Mechanisms Underlying Myalgic Encephalomyelitis/Chronic Fatigue Syndrome. *Diagnostics* **2019**, *9*, 80. [[CrossRef](#)]
7. Aaron, L.A.; Burke, M.M.; Buchwald, D. Overlapping conditions among patients with chronic fatigue syndrome, fibromyalgia, and temporomandibular disorder. *Arch. Intern. Med.* **2000**, *160*, 221–227. [[CrossRef](#)]
8. Giloteaux, L.; Goodrich, J.K.; Walters, W.A.; Levine, S.M.; Ley, R.E.; Hanson, M.R. Reduced diversity and altered composition of the gut microbiome in individuals with myalgic encephalomyelitis/chronic fatigue syndrome. *Microbiome* **2016**, *4*, 30. [[CrossRef](#)]
9. Nagy-Szakal, D.; Williams, B.L.; Mishra, N.; Che, X.; Lee, B.; Bateman, L.; Klimas, N.G.; Komaroff, A.L.; Levine, S.; Montoya, J.G.; et al. Fecal metagenomic profiles in subgroups of patients with myalgic encephalomyelitis/chronic fatigue syndrome. *Microbiome* **2017**, *5*, 44. [[CrossRef](#)]
10. Armstrong, C.W.; McGregor, N.R.; Lewis, D.P.; Butt, H.L.; Gooley, P.R. The association of fecal microbiota and fecal, blood serum and urine metabolites in myalgic encephalomyelitis/chronic fatigue syndrome. *Metabolomics* **2016**, *13*, 8. [[CrossRef](#)]
11. Guo, C.; Che, X.; Briese, T.; Ranjan, A.; Allicock, O.; Yates, R.A.; Cheng, A.; March, D.; Hornig, M.; Komaroff, A.L.; et al. Deficient butyrate-producing capacity in the gut microbiome is associated with bacterial network disturbances and fatigue symptoms in ME/CFS. *Cell Host Microbe* **2023**, *31*, 288–304.e288. [[CrossRef](#)] [[PubMed](#)]
12. Xiong, R.; Gunter, C.; Fleming, E.; Vernon, S.D.; Bateman, L.; Unutmaz, D.; Oh, J. Multi-omics of gut microbiome-host interactions in short- and long-term myalgic encephalomyelitis/chronic fatigue syndrome patients. *Cell Host Microbe* **2023**, *31*, 273–287.e275. [[CrossRef](#)] [[PubMed](#)]
13. Maes, M.; Mihaylova, I.; Leunis, J.C. Increased serum IgA and IgM against LPS of enterobacteria in chronic fatigue syndrome (CFS): Indication for the involvement of gram-negative enterobacteria in the etiology of CFS and for the presence of an increased gut-intestinal permeability. *J. Affect. Disord.* **2007**, *99*, 237–240. [[CrossRef](#)] [[PubMed](#)]
14. Shukla, S.K.; Cook, D.; Meyer, J.; Vernon, S.D.; Le, T.; Clevidence, D.; Robertson, C.E.; Schrodi, S.J.; Yale, S.; Frank, D.N. Changes in Gut and Plasma Microbiome following Exercise Challenge in Myalgic Encephalomyelitis/Chronic Fatigue Syndrome (ME/CFS). *PLoS ONE* **2015**, *10*, e0145453. [[CrossRef](#)] [[PubMed](#)]
15. Duchmann, R.; Neurath, M.F.; Meyer zum Büschenfelde, K.H. Responses to self and non-self intestinal microflora in health and inflammatory bowel disease. *Res. Immunol.* **1997**, *148*, 589–594. [[CrossRef](#)] [[PubMed](#)]
16. Harmsen, H.J.; Pouwels, S.D.; Funke, A.; Bos, N.A.; Dijkstra, G. Crohn's disease patients have more IgG-binding fecal bacteria than controls. *Clin. Vaccine Immunol.* **2012**, *19*, 515–521. [[CrossRef](#)] [[PubMed](#)]
17. Ruff, W.E.; Greiling, T.M.; Kriegel, M.A. Host-microbiota interactions in immune-mediated diseases. *Nat. Rev. Microbiol.* **2020**, *18*, 521–538. [[CrossRef](#)] [[PubMed](#)]
18. Maes, M.; Ringel, K.; Kubera, M.; Anderson, G.; Morris, G.; Galecki, P.; Geffard, M. In myalgic encephalomyelitis/chronic fatigue syndrome, increased autoimmune activity against 5-HT is associated with immuno-inflammatory pathways and bacterial translocation. *J. Affect. Disord.* **2013**, *150*, 223–230. [[CrossRef](#)]
19. Quigley, E.M. Gut bacteria in health and disease. *Gastroenterol. Hepatol.* **2013**, *9*, 560–569.
20. Keyt, B.A.; Baliga, R.; Sinclair, A.M.; Carroll, S.F.; Peterson, M.S. Structure, Function, and Therapeutic Use of IgM Antibodies. *Antibodies* **2020**, *9*, 53. [[CrossRef](#)]
21. de Sousa-Pereira, P.; Woof, J.M. IgA: Structure, Function, and Developability. *Antibodies* **2019**, *8*, 57. [[CrossRef](#)] [[PubMed](#)]
22. Vogl, T.; Kalka, I.N.; Klompus, S.; Leviatan, S.; Weinberger, A.; Segal, E. Systemic antibody responses against human microbiota flagellins are overrepresented in chronic fatigue syndrome patients. *Sci. Adv.* **2022**, *8*, eabq2422. [[CrossRef](#)] [[PubMed](#)]
23. Vogl, T.; Klompus, S.; Leviatan, S.; Kalka, I.N.; Weinberger, A.; Wijmenga, C.; Fu, J.; Zhernakova, A.; Weersma, R.K.; Segal, E. Population-wide diversity and stability of serum antibody epitope repertoires against human microbiota. *Nat. Med.* **2021**, *27*, 1442–1450. [[CrossRef](#)] [[PubMed](#)]
24. Conrey, P.E.; Denu, L.; O'Boyle, K.C.; Rozich, I.; Green, J.; Maslanka, J.; Lubin, J.B.; Duranova, T.; Haltzman, B.L.; Gianchetti, L.; et al. IgA deficiency destabilizes homeostasis toward intestinal microbes and increases systemic immune dysregulation. *Sci. Immunol.* **2023**, *8*, eade2335. [[CrossRef](#)] [[PubMed](#)]
25. Doron, I.; Leonardi, I.; Li, X.V.; Fiers, W.D.; Semon, A.; Bialt-DeCelie, M.; Migaud, M.; Gao, I.H.; Lin, W.Y.; Kusakabe, T.; et al. Human gut mycobiota tune immunity via CARD9-dependent induction of anti-fungal IgG antibodies. *Cell* **2021**, *184*, 1017–1031.e1014. [[CrossRef](#)] [[PubMed](#)]

26. Fadlallah, J.; Sterlin, D.; Fieschi, C.; Parizot, C.; Dorgham, K.; El Kafsi, H.; Autaa, G.; Ghillani-Dalbin, P.; Juste, C.; Lepage, P.; et al. Synergistic convergence of microbiota-specific systemic IgG and secretory IgA. *J. Allergy Clin. Immunol.* **2019**, *143*, 1575–1585. [\[CrossRef\]](#) [\[PubMed\]](#)
27. Koch, M.A.; Reiner, G.L.; Lugo, K.A.; Kreuk, L.S.; Stanbery, A.G.; Ansaldo, E.; Seher, T.D.; Ludington, W.B.; Barton, G.M. Maternal IgG and IgA Antibodies Dampen Mucosal T Helper Cell Responses in Early Life. *Cell* **2016**, *165*, 827–841. [\[CrossRef\]](#)
28. Rengarajan, S.; Knoop, K.A.; Rengarajan, A.; Chai, J.N.; Grajales-Reyes, J.G.; Samineni, V.K.; Russler-Germain, E.V.; Ranganathan, P.; Fasano, A.; Sayuk, G.S.; et al. A Potential Role for Stress-Induced Microbial Alterations in IgA-Associated Irritable Bowel Syndrome with Diarrhea. *Cell Rep. Med.* **2020**, *1*, 100124. [\[CrossRef\]](#)
29. Sterlin, D.; Larsen, M.; Fadlallah, J.; Parizot, C.; Vignes, M.; Autaa, G.; Dorgham, K.; Juste, C.; Lepage, P.; Aboab, J.; et al. Perturbed Microbiota/Immune Homeostasis in Multiple Sclerosis. *Neurol. Neuroimmunol. Neuroinflamm.* **2021**, *8*, e997. [\[CrossRef\]](#)
30. Vujkovic-Cvijin, I.; Welles, H.C.; Ha, C.W.Y.; Huq, L.; Mistry, S.; Brenchley, J.M.; Trinchieri, G.; Devkota, S.; Belkaid, Y. The systemic anti-microbiota IgG repertoire can identify gut bacteria that translocate across gut barrier surfaces. *Sci. Transl. Med.* **2022**, *14*, eab13927. [\[CrossRef\]](#)
31. Jackson, M.A.; Pearson, C.; Ilott, N.E.; Huus, K.E.; Hegazy, A.N.; Webber, J.; Finlay, B.B.; Macpherson, A.J.; Powrie, F.; Lam, L.H. Accurate identification and quantification of commensal microbiota bound by host immunoglobulins. *Microbiome* **2021**, *9*, 33. [\[CrossRef\]](#)
32. Gacesa, R.; Kurilshikov, A.; Vich Vila, A.; Sinha, T.; Klaassen, M.A.Y.; Bolte, L.A.; Andreu-Sánchez, S.; Chen, L.; Collij, V.; Hu, S.; et al. Environmental factors shaping the gut microbiome in a Dutch population. *Nature* **2022**, *604*, 732–739. [\[CrossRef\]](#) [\[PubMed\]](#)
33. Redondo-Useros, N.; Nova, E.; González-Zancada, N.; Díaz, L.E.; Gómez-Martínez, S.; Marcos, A. Microbiota and Lifestyle: A Special Focus on Diet. *Nutrients* **2020**, *12*, 1776. [\[CrossRef\]](#) [\[PubMed\]](#)
34. Lupo, G.F.D.; Rocchetti, G.; Lucini, L.; Lorusso, L.; Manara, E.; Bertelli, M.; Puglisi, E.; Capelli, E. Potential role of microbiome in Chronic Fatigue Syndrome/Myalgic Encephalomyelitis (CFS/ME). *Sci. Rep.* **2021**, *11*, 7043. [\[CrossRef\]](#) [\[PubMed\]](#)
35. Klein, S.L.; Flanagan, K.L. Sex differences in immune responses. *Nat. Rev. Immunol.* **2016**, *16*, 626–638. [\[CrossRef\]](#) [\[PubMed\]](#)
36. Milan-Mattos, J.C.; Anibal, F.F.; Perseguini, N.M.; Minatel, V.; Rehder-Santos, P.; Castro, C.A.; Vasilceac, F.A.; Mattiello, S.M.; Faccioli, L.H.; Catai, A.M. Effects of natural aging and gender on pro-inflammatory markers. *Braz. J. Med. Biol. Res.* **2019**, *52*, e8392. [\[CrossRef\]](#) [\[PubMed\]](#)
37. Vujkovic-Cvijin, I.; Sklar, J.; Jiang, L.; Natarajan, L.; Knight, R.; Belkaid, Y. Host variables confound gut microbiota studies of human disease. *Nature* **2020**, *587*, 448–454. [\[CrossRef\]](#) [\[PubMed\]](#)
38. Lax, S.; Smith, D.P.; Hampton-Marcell, J.; Owens, S.M.; Handley, K.M.; Scott, N.M.; Gibbons, S.M.; Larsen, P.; Shogan, B.D.; Weiss, S.; et al. Longitudinal analysis of microbial interaction between humans and the indoor environment. *Science* **2014**, *345*, 1048–1052. [\[CrossRef\]](#)
39. Guenther, S.; Loebel, M.; Mooslechner, A.A.; Knops, M.; Hanitsch, L.G.; Grabowski, P.; Wittke, K.; Meisel, C.; Unterwalder, N.; Volk, H.D.; et al. Frequent IgG subclass and mannose binding lectin deficiency in patients with chronic fatigue syndrome. *Hum. Immunol.* **2015**, *76*, 729–735. [\[CrossRef\]](#)
40. Aiello, A.; Farzaneh, F.; Candore, G.; Caruso, C.; Davinelli, S.; Gambino, C.M.; Ligotti, M.E.; Zareian, N.; Accardi, G. Immunosenescence and Its Hallmarks: How to Oppose Aging Strategically? A Review of Potential Options for Therapeutic Intervention. *Front. Immunol.* **2019**, *10*, 2247. [\[CrossRef\]](#)
41. Eaton-Fitch, N.; du Preez, S.; Cabanas, H.; Staines, D.; Marshall-Gradisnik, S. A systematic review of natural killer cells profile and cytotoxic function in myalgic encephalomyelitis/chronic fatigue syndrome. *Syst. Rev.* **2019**, *8*, 279. [\[CrossRef\]](#) [\[PubMed\]](#)
42. Naviaux, R.K.; Naviaux, J.C.; Li, K.; Bright, A.T.; Alaynick, W.A.; Wang, L.; Baxter, A.; Nathan, N.; Anderson, W.; Gordon, E. Metabolic features of chronic fatigue syndrome. *Proc. Natl. Acad. Sci. USA* **2016**, *113*, E5472–E5480. [\[CrossRef\]](#)
43. Morris, G.; Maes, M.; Berk, M.; Puri, B.K. Myalgic encephalomyelitis or chronic fatigue syndrome: How could the illness develop? *Metab. Brain Dis.* **2019**, *34*, 385–415. [\[CrossRef\]](#)
44. Schlomann, B.H.; Parthasarathy, R. Timescales of gut microbiome dynamics. *Curr. Opin. Microbiol.* **2019**, *50*, 56–63. [\[CrossRef\]](#)
45. Baker, R.; Shaw, E.J. Diagnosis and management of chronic fatigue syndrome or myalgic encephalomyelitis (or encephalopathy): Summary of NICE guidance. *BMJ* **2007**, *335*, 446–448. [\[CrossRef\]](#) [\[PubMed\]](#)
46. Fukuda, K.; Straus, S.E.; Hickie, I.; Sharpe, M.C.; Dobbins, J.G.; Komaroff, A. The chronic fatigue syndrome: A comprehensive approach to its definition and study. International Chronic Fatigue Syndrome Study Group. *Ann. Intern. Med.* **1994**, *121*, 953–959. [\[CrossRef\]](#) [\[PubMed\]](#)
47. Lewis, S.J.; Heaton, K.W. Stool form scale as a useful guide to intestinal transit time. *Scand. J. Gastroenterol.* **1997**, *32*, 920–924. [\[CrossRef\]](#)
48. Grüning, B.; Dale, R.; Sjödin, A.; Chapman, B.A.; Rowe, J.; Tomkins-Tinch, C.H.; Valieris, R.; Köster, J. Bioconda: Sustainable and comprehensive software distribution for the life sciences. *Nat. Methods* **2018**, *15*, 475–476. [\[CrossRef\]](#) [\[PubMed\]](#)
49. Telatin, A.; Fariselli, P.; Birolo, G. SeqFu: A Suite of Utilities for the Robust and Reproducible Manipulation of Sequence Files. *Bioengineering* **2021**, *8*, 59. [\[CrossRef\]](#) [\[PubMed\]](#)
50. Chen, S.; Zhou, Y.; Chen, Y.; Gu, J. fastp: An ultra-fast all-in-one FASTQ preprocessor. *Bioinformatics* **2018**, *34*, i884–i890. [\[CrossRef\]](#)
51. Wood, D.E.; Lu, J.; Langmead, B. Improved metagenomic analysis with Kraken 2. *Genome Biol.* **2019**, *20*, 257. [\[CrossRef\]](#) [\[PubMed\]](#)
52. Lu, J.; Breitwieser, F.P.; Thielen, P.; Salzberg, S.L. Bracken: Estimating species abundance in metagenomics data. *PeerJ Comput. Sci.* **2017**, *3*, e104. [\[CrossRef\]](#)

53. Oksanen, J.; Simpson, G.L.; Blanchet, F.G.; Kindt, R.; Legendre, P.; Minchin, P.R.; O'Hara, R.B.; Solymos, P.; Stevens, M.H.H.; Szoecs, E.; et al. *vegan: Community Ecology Package*, R package version v.2.6-4; 2022. Available online: <https://cran.r-project.org/web/packages/vegan/> (accessed on 21 March 2023).
54. Beghini, F.; McIver, L.J.; Blanco-Míguez, A.; Dubois, L.; Asnicar, F.; Maharjan, S.; Mailyan, A.; Manghi, P.; Scholz, M.; Thomas, A.M.; et al. Integrating taxonomic, functional, and strain-level profiling of diverse microbial communities with bioBakery 3. *Elife* **2021**, *10*, e65088. [[CrossRef](#)] [[PubMed](#)]
55. McIver, L.J.; Abu-Ali, G.; Franzosa, E.A.; Schwager, R.; Morgan, X.C.; Waldron, L.; Segata, N.; Huttenhower, C. bioBakery: A meta'omic analysis environment. *Bioinformatics* **2018**, *34*, 1235–1237. [[CrossRef](#)] [[PubMed](#)]
56. van den Boogaart, K.G.; Tolosana-Delgado, R.; van den Boogaart, M.B.K.G. *compositions: Compositional Data Analysis*, R package version 2.0-6; 2023. Available online: <https://cran.r-project.org/web/packages/compositions/> (accessed on 21 March 2023).
57. Rohart, F.; Gautier, B.; Singh, A.; KA, L.C. mixOmics: An R package for 'omics feature selection and multiple data integration. *PLoS Comput. Biol.* **2017**, *13*, e1005752. [[CrossRef](#)]
58. Wickham, H. *ggplot2: Elegant Graphics for Data Analysis*; Springer: New York, NY, USA, 2016.
59. Wickham, H. Reshaping Data with the reshape Package. *J. Stat. Softw.* **2007**, *21*, 1–20. [[CrossRef](#)]
60. Dowle, M.; Srinivasan, A.; Short, T. *data.table: Extension of 'data.frame'*, R package version 1.14.6; 2022. Available online: <https://cran.r-project.org/web/packages/data.table/> (accessed on 21 March 2023).
61. Wickham, H.; François, R.; Henry, L.; Müller, K.; Vaughan, D. *dplyr: A Grammar of Data Manipulation*, R package version 1.1.0; 2023. Available online: <https://cran.r-project.org/web/packages/dplyr/> (accessed on 21 March 2023).
62. Kassambara, A. *ggpubr: 'ggplot2' Based Publication Ready Plots*, R package version 0.6.0; 2023. Available online: <https://cran.r-project.org/web/packages/ggpubr/index.html> (accessed on 21 March 2023).
63. Grinnon, S.T.; Miller, K.; Marler, J.R.; Lu, Y.; Stout, A.; Odenkirchen, J.; Kunitz, S. National Institute of Neurological Disorders and Stroke Common Data Element Project—Approach and methods. *Clin. Trials* **2012**, *9*, 322–329. [[CrossRef](#)]

Disclaimer/Publisher's Note: The statements, opinions and data contained in all publications are solely those of the individual author(s) and contributor(s) and not of MDPI and/or the editor(s). MDPI and/or the editor(s) disclaim responsibility for any injury to people or property resulting from any ideas, methods, instructions or products referred to in the content.